Effect of process variables on the synthesis of MgB$_2$ by high energy ball mill

Haldun Kurama*, Savas Erkus*, Hakan Gasan**

*   Eskişehir Osmangazi University, Department of Mining Engineering, 26480, Eskişehir, Turkey.
    Corresponding author: hkurama@ogu.edu.tr (Haldun Kurama)
** Eskişehir Osmangazi University, Department of Metallurgical Engineering, 26480, Eskişehir, Turkey

Abstract: Discovery of superconductivity of MgB$_2$ with a critical temperature of -234 °C has offered the promise of important large-scale applications. Except for the other featured synthesis methods, mechanical activation, performed by high-energy ball mills to synthesis of bulk form of MgB$_2$ or as a first step of wire and thin film production has considered as an effective alternative production route in recent years. The aim of the present study was to determine the effect of process variables such as the ball-to-powder weight ratio (BPR), size of ball, milling time, annealing temperature and contribution of process control agent (toluene) on the product size, morphology and conversion level of precursor powders to MgB$_2$ after subsequent heat treatment. Although, the test results revealed relatively lower weight percent of MgB$_2$ phase formation compared with the literature, the reduced milling time, BPR and sinterability of pre-alloyed powder to MgB$_2$ at lowered temperature (630 °C) enhanced the applicability of mechanical alloying with SPEX mill.

Introduction

Superconductivity can be defined as a losing of all electrical resistance of either an element or metallic alloy when the material is cooled below a characteristic critical temperature. Superconductivity was discovered in 1911, and then greatly expanded with finding many superconductor forms (Tobin, 2008). The discovery of the superconductivity of MgB$_2$ with the critical temperature of -234 °C (39 K) has offered the promise of important large-scale applications at around -253 °C (20 K) (Nagamatsu et al., 2001). Specifically, a lack of weak-links at the grain boundaries, relatively high-critical temperature (T_c) of -234 °C (39 K), improved critical current density (J_c) and the low cost of the starting materials have made MgB$_2$ a promising candidate for wide range of practical applications. However, observed rapid drops of J_c at increased magnetic field indicated that the pristine MgB$_2$ still exhibited

deteriorated superconductivity properties (Sergey, 2007). It was suggested that the lack of defects as flux-pinning centers was responsible for this rapid decline. Therefore, later studies, such as element doping and nanoparticle addition, were mainly focused on increasing the flux pinning to enhancement of J_c and modifying the superconducting properties while maintaining high T_c. In these studies, chemical doping with carbon containing compounds such as SiC (Due et al., 2004; Kumara et al., 2004; Sumption et al., 2005; Matsumoto et al., 2006), C (Pranthaman et al., 2001; Wilke et al., 2004; Yan et al, 2008) and carbon nanotubes (Kim et al., 2006) have been considered as one of the promising methods to enhance J_c. However, the achievements from these routes were found to be limited because of decreased superconducting volume, degradation of connectivity, agglomeration of nanosized doping materials and poor reactivity between boron and carbon (Lee et al., 2009). Except that the partial substitution, mechanical activation or alloying methods, which have been performed to synthesis of bulk form MgB_2 or used as a first step of wire or thin film productions, have also been considered as an effective alternative production way by several researchers. It is well-known that the purity of the precursor powers and the grain size are the crucial parameters for the superconducting properties of MgB_2. A microstructure with very small sized defects is the favorable condition for the optimum pinning of magnetic flux lines (Ribeiro et al., 2003). The effect of precursor powder purity was well discussed previously by Zhou et al. (2004). The authors showed that the purity of the B powder had strong effect on T_c and J_c of the MgB_2. It was found that amorphous boron samples made from different purities exhibited different J_c, and also that the highest purity boron (99.99%) yielded the highest J_c. This was mainly attributed to the impurity phases (mainly MgO and B_2O_3) present in the product. Oxidation of impurities and decrease in the superconductor volume led to drop of this value. On the other hand, for the effect of particle size, it was recognized that the low purity boron powders produce lower surface reactivity and larger particle size than the high purity boron powder usage. Therefore, J_c of the product decreased in comparison to MgB_2 produced from the high purity boron powder.

Mechanical alloying (MA) is a solid-state powder processing technique that involves repeated cold welding, fracturing and re-welding of powder particles in a high-energy ball mill (Suryanarayana, 2001). These actions facilitate formation of an optimal microstructure with particle sizes of several nanometers. During MA, heavy deformation is introduced into the particles. This is manifested by the presence of a variety of crystal defects such as dislocations, vacancies, stacking faults and increased number of grain boundaries. The presence of this defect structure enhances the diffusivity of solute. Therefore, MgB_2 synthesis with MA has been applied for improving the critical currents and magnetic flux pinning ability of the product due to enhanced grain boundary density resulting from decreased grain size and increased crystal defects. Gumbel et al. (2002, 2003) reported that high density nanocrystalline MgB_2 bulk superconductors with improved pinning could be prepared by mechanical alloying of Mg and B powders at ambient temperatures followed by hot

pressing. MA was performed in a planetary ball mill with using high quality amorphous B (99.9 wt %) and Mg (99.8 wt %) powders at the BPR of 36:1. The results confirmed that such powder consist of nanocrystalline grains and was very reactive for alloying. It was also found that the superconducting transition temperature decreased with increasing milling time from -237.25 °C (35.9 K) for 20 h to -242.35 °C (30.8 K) for 100 h. The most favorable conditions were determined as milling time between 20 and 50 h, followed by hot pressing at 700 °C (973 K). A similar technique was also used by Haßler et al. (2003, 2006) in order to investigate the influence of the quality of boron precursor powder on the microstructure and superconducting properties of MgB$_2$ bulk samples and tapes. Preparation of bulk samples was performed by using elemental high grade Mg and amorphous B powder with BPR of 36:1. Mechanical alloying was realized in a planetary mill for 50 h at ambient temperature with rotation speed of 250 rpm. It was reported that the precursor powder with 20–60 nm was highly reactive and tapes could be prepared at relatively low temperatures (500–600 °C) by a powder-in-tube technique. Perner et al. (2004) investigated the effect of microstructure and chemical composition variations on the formation of MgB$_2$. The samples were synthesized by using planetary mill and the milled powder was then subsequently hot pressed. According to the morphological and chemical analyses, the authors suggested that the maximum pinning force increased first with increasing milling time, reaching its largest value of nearly 8×10^8 N m^{-3} for 30 and 50 h milled samples. The decreased grain size and the increased content of W, C, Co and O impurities with increasing milling time were attributed to the main affects for the drop of pinning force. Oxygen was found as the strongest impurity, it was trapped during the different preparation steps because of the clean and highly reactive surfaces of the powder particles even high purity inert gas were used. Consequently, although some alternative routes such as usage of a magneto-Uni-Ball-Mill and electrical discharge in mechanical alloying (Varin et al, 2004, 2006) or attrition ball mill followed by heat treatment (Lee et al, 2009) were offered, most of the researches have been performed by using planetary mills with a relatively higher milling time and higher BPRs. In MA, even though the linear velocity of the balls in the planetary type of mill is higher than that in the SPEX mill, the frequency of impacts is much more in the SPEX mills. Hence, in comparison to SPEX mills, planetary mills can be considered as lower energy mills. The time required for processing is generally shorter in SPEX mills and longer in either attritors or planetary mills. The back-and-forth shaking motion is combined with lateral movements of the ends of the vial. With each swing of the vial, the balls impact against the sample, hence, at the end of the movement, both milling and mixing of the sample has been provided. Due to the amplitude equal to about 5 cm and speed about 1200 rpm of the clamp motion, the ball velocities are high (5 m/s), and consequently the force of the ball impact is unusually great (Suryanarayana, 2001). Therefore, compared to planetary mill, it is possible to obtain homogeneous nano-sized MgB$_2$ in the milling stage with relatively shorter milling time. The occurred heavy deformation during

milling can also leads to increasing the number of grain boundaries with a variety of crystal defects. This defect structure enhances the diffusivity of solute. As briefly discussed above, for the planetary mills, the optimum milling time was determined as between 20 and 50 h, however, for the SPEX mill it was only 2-5 h. Additionally, it has been recognized that this technique can be used to induce chemical reactions due to generation of clean and fresh surfaces (a result of fracturing), increased defect density and reduction of particle sizes. This allows to production of nonosized intermetalic grains during milling at much lower temperatures than normally required to synthesize pure metals or alloys. The performed pre-alloying in the milling stage positively affects crystallization of target compound in further heat treatment. The study performed by Wu et al. (2007), with using the SPEX mill showed that a bulk form of MgB_2 with improved magnetization properties could be synthesized in a relatively short time. It was reported that the highest J_c, approximately $2.3 \cdot 10^5$ A/cm^2 (-258.15 °C =15 K, 3 T) could be obtained for the samples milled for 5 h and sintered at 750 °C for 1 h. This result was found very encourageable for the further studies, which concern synthesis of MgB_2 by a high-energy ball milling method at relatively lower temperatures. However, due to complexity of MA, the effect of process variables on the final product properties such as size of balls, ball-to-powder weight ratio and introduction of process control agents during milling still needs identification. Therefore, the aim of the present study is focused only on determination of the effect of these parameters on the product size, morphology and conversion level of precursor powders to MgB_2 during milling and after subsequent heat treatment.

Experimental

MgB_2 was synthesized by a following in-situ reaction process. Preparation of the powder was carried out with elemental Mg (99.8 wt% purity, less than 45 μm particle size) and amorphous B (95 wt% purity, 1 μm particle size) powders mixed in the stoichiometric ratio of MgB_2 with 5 wt.% Mg surplus in tungsten carbide (WC) vials filled with WC balls in purified argon atmosphere to avoid oxidation. The milling was performed in the SPEX 8000D mill for different time intervals of 2, 4 and 6 h. The milling of the powders was performed at BPRs of 3 and 6 with using WC balls with diameters of 11.2 mm, 11.2 + 5 mm and 5 mm. The well mixed powders were mechanically cold-pressed into a pellet of 29 mm in diameter and 4 mm in thickness under a pressure of 1 GPa, and then immediately placed in an alumina crucible and heat-treated inside a tube furnace under ultra-high purity Ar-atmosphere. The synthesis temperatures were particularly chosen according to TG analyses of milled powder to get optimal parameters.

The phase compositions of the samples were performed with an S5000 diffractometer, with nickel filtered Cu Kα radiation. The surface morphology and microstructures of the samples were characterized by using a high vacuum electron microscope ZEISS SUPRA VP 50. For the Rietveld refinement, X-ray diffraction

(XRD) patterns were analyzed by the Sleve+ 2015 search indexing software, with reference to the patterns of the PDF-4+ 2015 database. All phases were identified semi-automatically by taking into consideration the Goodness-of-Match values and crystallographic information files (CIFs) were downloaded from the database for the MgO and the MgB$_2$ phases. The Rietveld refinement technique was applied by using the MAUD (materials analysis using diffraction) program, which was designed to simultaneously refine the material structure and microstructure through the Marquardt least-squares method. The shape of the peaks was modeled by a pseudo-Voigt function. Refinement continued until convergence was reached in each step with a goodness of fit (GOF) close to 1.

The thermal behavior of the mechanically alloyed precursor powder was investigated by a TG-TGA technique under argon atmosphere with a heating rate of 20 K min^{-1} (-253.15 °C min^{-1}) using a NETZSCH STA 409 PC/PC instrument. Particle size distributions of the milled samples were performed by a Malvern particle size analyzer 2000. To ensure reliable data acquisition, the powders were ultrasonically dispersed in water to avoid agglomeration of powder particles.

Results and discussion

Phase transformation of MgB$_2$ sample

The TG–DTA curve of the milled sample is given in Figure 1. It shows series of characteristic exothermic peaks. The first peak at 529 °C can be attributed the reaction between free Mg and B. The exotherm in the temperature range 580–620 °C is due to partial oxidation of the sample and formation of magnesium oxide as previously evidenced by Lomovsky et al. (2010). The third stronger peak observed at 688 °C, which starts at approx. 630 °C and ends at near 700 °C is corresponded to formation of MgB$_2$ phases. This effect was used for the determination of annealing conditions.
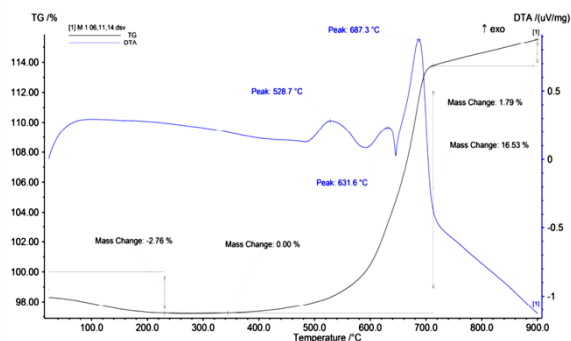

Fig. 1. TG-DTA curve of milled sample with 11.2 mm balls,
2 h milling, sintered at 630 °C at 2 h with argon flow rate of 10 cm³/min

Phase composition analysis

Effect of argon flow rate on MgB$_2$ phase composition during sintering

The XRD patterns of the samples milled for 2 h and sintered in tube furnace at 630 °C for 2 h under argon atmosphere with flow rates of 1, 3 and 5 cm^3/min are given in Fig. 2. Although the intensity of XRD patterns slightly changed with applied argon flow rates, it was found that for all cases, the main peaks of MgB$_2$ were clearly visible together with little amounts of MgO peaks. It revealed the occurrence of MgB$_2$ as relatively pure form at lower temperature and the BPR ratio.
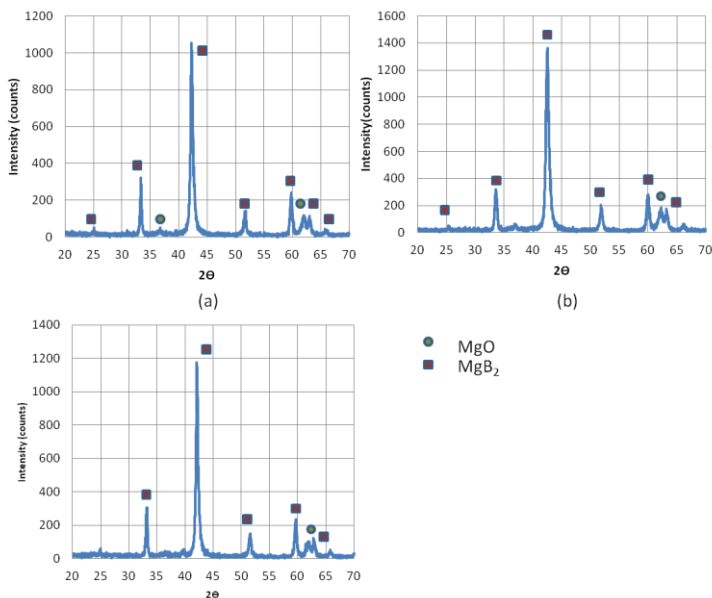

Fig. 2. XRD patterns of samples sintered with different argon flow rates,
(a) 1, (b) 3 and (c) 5 cm^3/min

Table 1. MgB$_2$ phase fraction variations according to applied argon flow rates. Milling conditions: 11 mm balls size, 2 h milling, sintering 2 h at 630 ^{o}C

Run	MgO, %	MgB$_2$, %	Argon flow rate, cm^3/min
1	19.84	80.16	1
2	16.64	83.36	3
3	13.71	86.29	5

On the other hand, the calculated conversion levels by the Rietveld refinement analyses (Table 1) indicated that the increased flow rate had a positive effect on the synthesis process. The wt % of MgB$_2$ phases increased with increasing argon flow rates. For the argon flow rate of 5 cm^3/ min, MgB$_2$ can be synthesized with 86 wt %.

The determined slight lower conversion can be attributed to higher impurity content of amorphous boron precursor and the reduced particle size during milling which lead to increasing of the oxidation reaction rate. The amorphous form of B powders has greater reactivity that the crystalline powders and their usage is reported elsewhere (Abe et al., 2003; Zhou et al., 2004; Chen et al., 2005; Zu et al., 2006). Nevertheless, the amorphous forms of B powders contain more B$_2$O$_3$ since they are fabricated by high-temperature Mg reduction of B$_2$O$_3$ as reported by Abe et al. (2003). The impurity content of the amorphous form of B powders with a different purity was analyzed (EDS analyses) by Zu et al. (2006) and it was shown that 96% boron powder consisted mainly of 96.38% B, 2.89% O, 0.16% Fe, 0.38% Mg, and little amounts of other impurities. The 99% pure boron consisted of only 1.74% of O.

The XRD pattern of amorphous boron powder used in experiment is given in Fig. 3. It shows crystalline peaks of B, despite being labeled as amorphous. Some possible B$_2$O$_3$ peaks were also marked together with B peaks. This result seems to be similar with the findings previously reported by Chen et al. (2005). The intensities of the possible B$_2$O$_3$ peaks analyzed for lower grade B-A9597 were found to be very low compared to B-A9999. It caused decreasing of the conversion level of B and Mg to MgB$_2$.
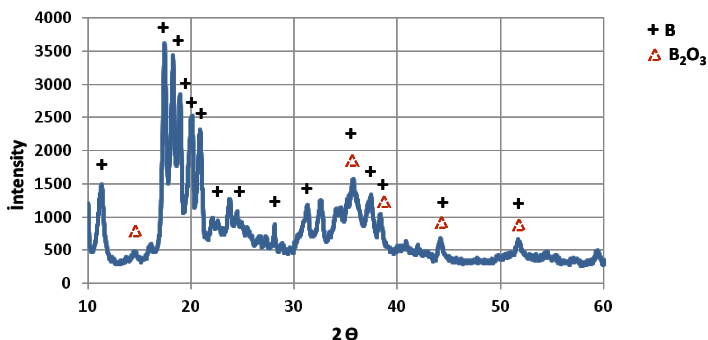

Fig. 3. XRD pattern of boron sample used in experiments

Effect of milling time and ball size

The effect of milling time and different balls sizes on formation of MgB$_2$ samples for the argon flow rate of 5 cm^3/min was evaluated based on the Rietveld refinement analyses (Fig. 4). As can be seen from Fig. 4-a, the MgB$_2$ phase wt % of the samples that were milled 2 h at BPR of 3:1 and heat treated at 630 °C during two hours, slightly increased with increasing milling time from 2 to 4 h. Nevertheless, the further increase in milling time up to 6 h slightly decreased formation of MgB$_2$phase content. It was also observed that the effect of different balls sizes was very limited for 2 h milling. The MgB$_2$ phase wt %, was calculated nearly 86% for the all ball sizes (Fig. 4b). However, this effect became more visible for the increased milling time to 6 h for 5 mm of balls. Under these conditions, the MgB$_2$ phase was calculated as 66.58%.

These facts can be attributed to either stability of the surface coating or agglomeration of particles at the beginning and also further stages of milling.
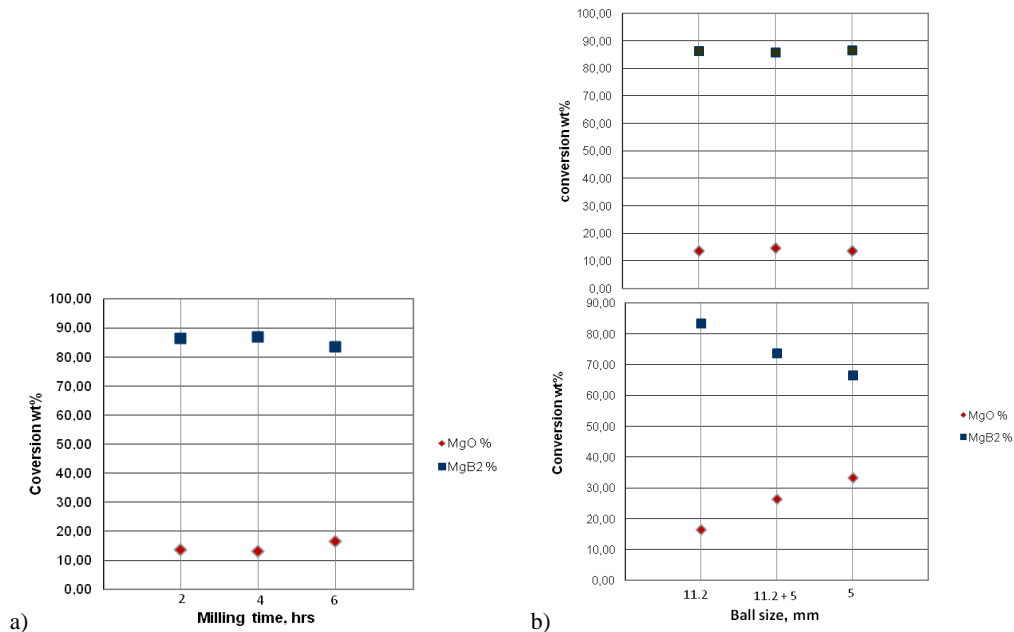

a)   b)

Fig. 4. MgB$_2$ phase wt % variation of samples according to different treatment times; 2, 4 and 6 h (a) and different size of balls for 2 and 6 h, respectively (b)
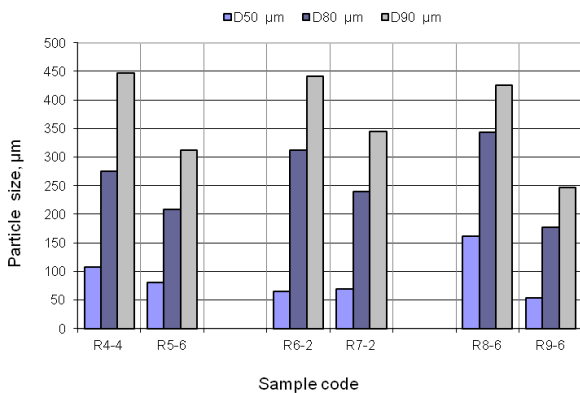

Fig. 5. Particle size distributions of samples milled with different ball sizes

In MA, most of the researches were generally performed by using only one size of the grinding medium; however, the highest collision energy can be obtained if the balls with different diameters were used (Gavrilov et al. 1995). This can be explained by production of shearing forces that may help in detaching the powder from the

surface of balls. In the initial stages of milling, some amount of milled powder is trapped between balls and coats onto the surface of the grinding medium and leads to cold welded of particles. With either continued deformation or milling, the particles get work hardened and fragmentation is occurred. Fragments generated by this mechanism may continue to reduce in size in the absence of strong agglomerating forces. At this stage, the tendency to fracture predominates over cold welding and narrow size distribution is obtained. Either surface coating or agglomeration of particle in each run may be advantageous since it prevents excessive wear of the grinding medium and avoids contamination of the powder due to the wear of the grinding medium. However, the thickness of this layer must be kept in a minimum to avoid formation of a heterogeneous final product. Furthermore as it can be seen in Fig. 5, the distribution of particle size for increased milling times, 4 and 6 h (R4-4 and R5-6), and combined (R6-2, 5+11.2 mm) or smallest ball usages (R7-2, 5mm) for 2 h and 6 h of milling times (R8-6 and R9-6) for the BPR of 3:1 exhibits heterogeneous distribution. This was assumed that the amount of powder mass at this ratio was too high. The higher powder weight led to increasing of the thickness of coating layer and agglomeration density between particles. Therefore, fragmentation of welded particles during the prolonging stages was reduced which limited the effects of different size ball usage. Although the size of the milled particles can be relatively reduced through the lower sizes with using lowest ball sizes (5 mm) at 6 h of milling compared to the ball size of 11.2 mm or mix usage, the size distribution pattern was still heterogeneous. Therefore, the reduction observed on the MgB₂ phase % for 6 h milling with using 5 mm balls (Fig. 4-b) can be explained by instability of the system which decreases the nucleation of small size particles to form crystalline MgB₂ compounds.

Effect of BPR and process control agent

Further experiments were performed at BPR of 6:1 and the usage of process control agent (toluene) was concerned to overcome the lower conversion levels of MgB₂ obtained in the previous part. The particle size measurement results of the samples performed with 11.2 mm ball at BPR of 6:1 during 2 and 6 h of milling (R5 and R10) indicated that only the reduction of BPR was not considerable effect on the product size even milled at 6 h compared to addition of toluene (Fig. 6). The milling process performed by 5 mm balls during 2 h (R12) resulted in increased homogeneity and lower particle size compared to 11.2 mm balls (R11). This result confirmed to previous findings reported by Xu et al. (2006). It was stated that milling boron powders with toluene effectively enhanced J_c. The value of J_c was estimated to be 5×10^3 A cm^{-2} at 8 T and 5 K (-268.15 °C). This value was found to be much higher than that of pure MgB₂ that was not milled. It was proposed that ball milling of B powders using with toluene led to smaller MgB₂ grains, resulting in enhanced J_c at low operating temperature and high field. As discussed above, during milling, the powder particles get cold-welded to each other, especially if they are ductile, powder particles plastically deforms due to force of impact. However, true alloying among powder

particles can occur only when a balance is maintained between cold welding and fracturing of particles. A process control agent is added to the powder mixture during milling to reduce the effect of cold welding. The agent adsorbs on the surface of the powder particles, minimizes cold welding between powder particles, and thereby inhibits agglomeration.
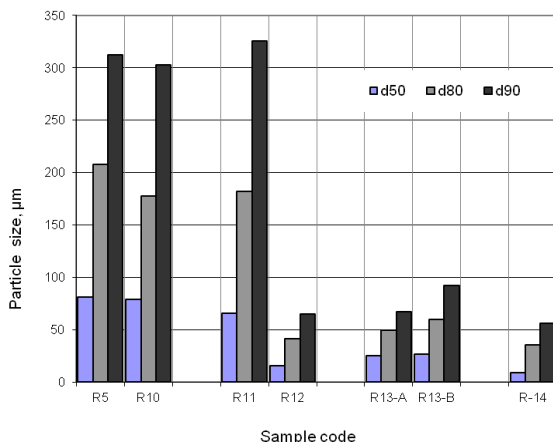

Fig. 6. Particle size measurement results of samples milled at BPR of 6:1
with toluene as a process control agent

In further tests, the boron powders were first milled with toluene for a period of 15 min, than Mg powders were added into the vials at BPR of 6:1, further milled at 2h with using 11.2 mm (R13-B) and 5 mm size balls (R13-A) respectively to observe the effect of toluene usage only for milling of boron powders before MA, as proposed by Kim et al. (2006). As can be seen in Fig. 6, the size of the milled product slightly decreased with using 5 mm balls. The same conclusion can be given also for R14, which represents the prolonged condition (6 h milling) of R12. The values of d_{90} of the sample R14 slightly decreased from 65 to 56 μm compared with R12.

Morphological analysis

The SEM image of the sintered form of sample R12, and the sample milled under the same condition but sintered at modified annealing is given in Fig. 7. According to the Rietveld refinement analyses of R12, it was found that the percentages of MgO increased from 13.71 to 32 %, while MgB_2 decreased from 86 to 67 wt % compared to R3. This result can be attributed to increased oxidation effect of toluene usage and also lowered particle size.
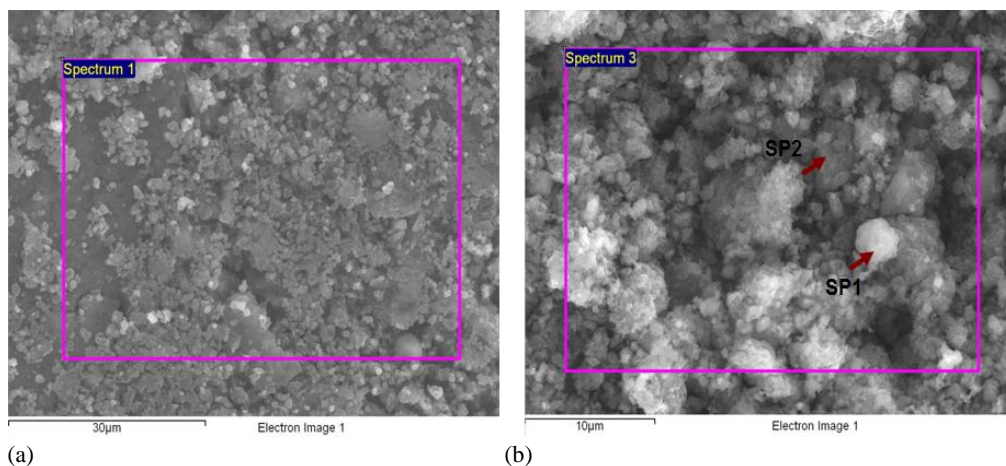
Figure 7 SEM images of sample R12 (a) and a sample sintered at modified annealing (b)

Toluene, C_7H_8, is an aromatic hydrocarbon and it does not contain any oxygen. Normally, it is expected that toluene is not harmful for the alloy system. It can only contribute to dispersion strengthening of the material resulting in increased strength and higher hardness. However, some earlier report indicated that hydrogen acted as a catalyst for amorphous phase formation in titanium-rich alloys (Ivison et al, 1992). Therefore, it might successes that not only the possible contribution of toluene, also the increased surface area and the activity of the particles lead oxidation of boron and magnesium. Li et al. (2009) showed that detection of B_2O_3 phases at the XRD spectrum of milled sample, even milled under Ar atmosphere, was attributed to reaction of boron with oxygen to form B_2O_3 as an impurity phase. This was explained by the storage of energy in the milled boron powders, and then mechanical deformation. During drying and heat treatment, this can improve the reactivity between boron and gaseous oxygen. Kim et al. (2006) stated that the impurity in the boron powder was present in the liquid state during MgB_2 formation, due to its low-melting temperature of 450 °C, which allowed it to react with magnesium to form MgO. In our study, although the XRD pattern of R12 does not show any distinct crystalline B_2O_3 peaks, the decreased intensity of MgB_2 and large dark grey area (spectrum 1) visible in SEM image (Fig. 7-a) indicates that the occurrence of amorphisation. It is well-known that the rate of amorphisation is faster during wet grinding than dry one. If the kinetic condition is unstable, MgB_2 compounds are difficult to nucleate, and an amorphous phase often nucleates. With further milling, the amount of the amorphous phase continues to increase through growth of the amorphous phase domains and/or through nucleation and growth of new amorphous phase domains.

In order to decrease the impurity level, further experiments were performed with employing of the modified annealing procedures. The pressed samples were subjected to heat treatment as the step-by-step mode. In the first step the temperature of furnace

was increased up to 450 °C by heating rate of 10°/min and the pressed samples were hold in furnace during 2, 4 and 8 hours. The furnace temperature increased to 630 $^{\circ}$C with the same heating rate and hold during 2 h.

Table 2. SEM-EDX results of selected samples

R12		R16		SP1[*]		SP2[**]	
Element	wt %	Element	wt %	Element	wt %	Element	wt %
Mg	27.47	Mg	26.15	Mg	37.86	Mg	22.17
B	15.20	B	53.64	B	18.13	B	60.22
C	1.41	C	-	C	2.31	C	-
O	55.72	O	19.89	O	41.70	O	17.20

[*] impurity (MgO) reach phase in light grey
[**] Boron reach phase in black

The Rietveld refinement analyses showed that holding at 450 $^{\circ}$C had a beneficial effect on the sample compositions. It was calculated that the wt % of MgO decreased from 32 to 21.77, 23.27 and 20.45%, while the wt % MgB_2 increased from 67 to 76.72, 78.23 and 79.55% respectively. The SEM images of sample R16 sintered at two stages, first annealing at 450 $^{\circ}$C during 8 h and further heat treated at 630 $^{\circ}$C during 2 h, is given in Fig. 7-b. It shows more homogeneous crystalline phases compared to previous one. The decreased impurity level could also be visible. Nevertheless, the conversion level of MgB_2 was still lower than the stoicheiometric value of 92%. The EDX analyses performed at selected points also confirmed the above findings (Table 2).

Conclusions

According to experimental tests results the following conclusions can be drawn.

Based on the Rietveld refinement analyses, the MgB_2 with an 87 wt % can be produced by using 11.2 mm balls, 2 h milling, BPR of 3:1 and sintered at 630 °C at 2 h under the argon flow rate of 5 cm^3/min. However, the particle size measurement revealed that the alloyed particles were coarse and showed heterogeneous distribution.

The effect of ball size or combined usage of coarse and fine balls was found to have a negligible effect on the particle size distribution and MgB_2 phase wt %. However, prolongation of the milling time to 6 h and use of fine balls had a strong effect on the formation MgB_2. The phase wt % decreased from 87% to 66%.

For increasing BPR from 3:1 to 6:1 the milling powders consisted of relatively finer grains but still exhibited heterogeneous distribution. On the other hand, the use of toluene as control agent during milling resulted in the homogeneous distribution and the milled powder consisted of finer particles even at applied short milling time (2 h). Nevertheless, it was analyzed that the sintered sample had higher impurities as oxide forms.

The performing of sintering stage as a step-by-step mode, first sintering at 450 °C during 8 h and later 2 h at 630 ^{o}C was found to be positively affected the decreasing of the impurity level, the MgB_2 phase wt % increased to approx. 80%.

Although, compared to the literature, relatively lower MgB_2 phase wt % were obtained, the reduced milling time, BPR and sinterability of pre-alloyed powder to MgB_2 at lowered temperature (630 ^{o}C) showed that MA with the SPEX mill could be concerned as a cost effective method especially for the industrial applications. However, these results should be supported with magnetization measurements.

Acknowledgements

Reference

TOBİN J.R., 2008, *Superconductivity Research Developments*, Nova Science Publishers, Inc. New York,

NAGAMATSU J., NAKAGAWA N., MURANAKA, T., ZENITANI Y., AKIMITSU J., 2001, *Superconductivity at 39K in magnesium diboride,* Nature 410, 63-64SERGEY L., 2007, *Recent advances in crystal growth of pure and chemically substituted MgB₂,* Physica C 456, 14–21

DOU S. X., BRACCINI V., SOLTANIAN S., KLIE R., ZHU Y., LI S., WANG X.L., LARBALESTIED C.R., 2004, *Nanoscale-SiC doping for enhancing J_c and H_{c2} in superconducting MgB2,* J. Appl. Phys. 96, 7549

KUMAKURA H., KITAGUCHI H., MATSUMOTO A., HATAKEYAMA H., 2004, *Upper critical fields of powder-in-tube-processed MgB₂/FeMgB₂/Fe tape conductors,* Appl. Phys. Lett. 84, 3669

SUMPTION M. D., BHATIA M., RINDFLEISCH M., TOMSIC M., SOLTANIAN S., DOU S. X., COLLINGS E. W., 2005, *Large upper critical field and irreversibility field in MgB2 wires with SiC additions,* Appl. Phys. Lett. 86, 092507

MATSUMOTO A., KUMAKURA H., KITAGUCHI H., SENKOWICZ B.J., JEWELL M.C., HELLSTROM E.E., ZHU Y., VOYLES P.M., LARBALESTIER D.C., 2006, *Evaluation of connectivity, flux pinning, and upper critical field contributions to the critical current density of bulk pure and SiC-alloyed MgB₂,* Appl. Phys. Lett. 89,132508

PARANTHAMAN J.R., THOMPSON D., CHRISTEN K., 2001, *Effect of carbon-doping in bulk superconducting MgB₂ sample,* Physica C 355, 1

WILKE R H.T., BUDKO S.L., CANFIELD P.C., FINNEMORE D.K., SUPLINSKAS R.J., HANNAHS S.T., 2004, *Systematic effects of carbon doping on the superconducting properties of Mg(B₁₋ₓ Cₓ)₂,* Phys. Rev. Lett. 92, 217003

YAN S.C., ZHOU L., YAN G., YANG Q.W., LU Y.F., 2008, *Effect of carbon doping on the formation and stability of MgB₂ phase,* J. Alloys Compd. 459, 452.

KIM J.H., YEOH W.K., XU X., DOU S.X., MUNROE P., RINDFLEISCH M., TOMSIC M., 2006, *Superconductivity of MgB₂ with embedded multiwall carbon nanotube,* Physica C 449, 133–138

LEE J. H., SHIN S. Y., KIM C. J., PARK H. W., 2009, *Superconducting properties of MgB₂ prepared from attrition ball-milled boron powder,* Journal of Alloys and Compounds 476, 919–924

RIBEIRO R.A., BUDKO S.L., PETROVIC C., CANFIELD P.C., 2003, *Effects of boron purity, Mg stoichiometry and carbon substitution on properties of polycrystalline MgB₂,* Physica C 385, 16–23

SURYANARAYANA C., 2001, *Mechanical alloying and milling,* Progress in Materials Science 46, 1-184

GUMBEL A., ECKERT J., FUCHS G., NENKOV K., MULLER K-H., SCHULTZ L., 2002, *Improved superconducting properties in nanocrystalline bulk MgB₂,* Appl. Phys. Lett. 80**,** 2725

GUMBEL A., PERNER O., ECKERT J., FUCHS G., NENKOV K., MULLER K-H, SCHULTZ L., 2003*, High density nanocrystalline MgB₂ bulk superconductors with improved pinning*, IEEE Trans. Appl. Supercond. 13**,** 3064

WAßLER W., RODIG. C, FISCHER C., HOLZAPFEL B., PERNER O., ECKERT J., NENKOV K., FUCHS G.*,* 2003*, Low temperature preparation of MgB₂ tapes using mechanically alloyed powder,* Supercond. Sci. Technol. 16, 281–284

WAßLER W., BIRAJDAR B., GRUNER W., HERRMANN M., PERNER O., RODIG C., SCHUBERT M., HOLZAPFEL B., EIBL O., SCHULTZ L.*,* 2006*, MgB₂ bulk and tapes prepared by mechanical alloying: influence of the boron precursor powder,* Supercond. Sci. Technol. 19, 512–520

PERNER O, ECKERT J., HAßLER W., FISCHER C., MULLER K-H., FUCHS G., HOLZAPFEL B., SCHULTZ L., 2004, *Microstructure and impurity dependence in mechanically alloyed nanocrystalline MgB₂ superconductors,* Supercond. Sci. Technol. 17, 1148

VARIN R.A., CHIU C.H., 2006, *Synthesis of nanocrystalline magnesium diboride (MgB₂) metallic superconductor by mechano-chemical reaction and post annealing,* J. Alloys Compd., 407, 268–273

VARIN R.A., CHIU C.H., LI S., CALKA A., WEXLER D., 2004, *Application of controlled and electrical discharge assisted mechanical alloying for the synthesis of nanocrystalline MgB₂ superconducting compound*, Journal of Alloys and Compounds 370, 230–243

LEE J.H., SHIN S.Y., KIM C.J., PARK H.W., *2009, Superconducting properties of MgB₂ prepared from attrition ball-milled boron powder,* Journal of Alloys and Compounds 476, 919–924

WU Y.F., LU Y.F., LI J.S., CHEN S.K., YAN G., PU M.H., LI C.S., ZHANG P.X., 2007, *The microstructures and superconducting properties of MgB2 bulks prepared by a high-energy milling method*, Physica C 467, 38–42

LOMOVSKY O.I., GOLUBKOVA G.V., DOVLİTOVA L.S., ZAİKOVSKII V.I., MALY V.I., 2010, *Mechanochemical synthesis of amorphous and crystalline magnesium diboride,* Inorganic Materials, 46, (1), 22–27

ABE H., NAITO M., NOGI K., MATSUDA M., MIYAKE M., OHAR A S., KONDO A., FUKUI T., 2003, *Low temperature formation of superconducting MgB₂ phase from elements by mechanical milling,* Physica C 391, 211–216

ZHOU S., PAN A.V., HORVAT J., QIN M.J., LIU H.K., 2004*, Effects of precursor powders and sintering processes on the superconducting properties of MgB₂* Supercond. Sci. Technol. 17, S528–S532

CHEN K, YATES KA., BLAMİRE M.G., MACMANUS-DRİSCOLL J.L., 2005, *Strong influence of boron precursor powder on the critical current density of MgB₂,* Supercond. Sci. Technol. 18**,** 1473–1477

XU X., QIN M.J., KONSTANTINOV K., DOS SANTOS D.I, YEOH, W.K. KIM J.H., DOU, S.X., 2006*, Effect of boron powder purity on superconducting properties of MgB₂,* Supercond. Sci. Technol. 19**,** 466–469

GAVRILOV D., VINOGRADOV O., SHAW W.J.D., 1995, *Simulation of mechanical alloying in a shaker ball mill with variable size particle*, Proc. Int. Conf. on Composite Materials, ICCM-10, Woodhead Publishing, 299-307

IVISON P.K, SOLETTA I, COWLAM N., COCCO G., ENZO S., BATTEZZATI L., 1992, *The effect of absorbed hydrogen on the amorphization of CuTi alloys*, J. Phys: Cond. Matter 4, 5239–5248